RSC Advances

ROYAL SOCIETY OF CHEMISTRY

www.rsc.org/advances

Analysis of slumping on nanoimprint patterning with pseudoplastic metal nanoparticle fluid

Li Dongxue[1], Su Yufeng[2], Xia Weiwei[1], Liu Chaoran[1], Wang Wen[1], Wang Pan[1], Duan zhiyong[1]*

(1.Physical Engineering College, Zhengzhou University, Zhengzhou, 450001, China.

2. Mechanical Engineering College, Zhengzhou University, Zhengzhou, 450001, China.

*. Corresponding author, duanzhiyong@zzu.edu.cn)

Abstract: Slump of patterning in the demolding process is a serious problem when pseudoplastic metal nanoparticle fluid is used as resist in nanoimprint, which adversely affects the fidelity of imprint patterning. A theoretical slumping model is proposed to study the influence of the shear-thinning of pseudoplastic fluid on the patterning. The conclusions showed that the critical viscosity increased with the increase of consistency coefficient or rheological index, decreased with the increase of surface tension coefficient, and was independent from density on the basis of the force analysis of microstructure at the end of demolding. Another conclusion was validated that larger demolding velocity led to greater extent of viscosity decrease. These results provide a theoretical reference for higher fidelity patterning in nanoimprint lithography with pseudoplastic metal nanoparticle fluid.

Keywords: nanoimprint, slumping, pseudoplastic metal nanoparticle fluid (PMNF), demolding, shear-thinning

1. Introduction

Chou et. al. proposed Nanoimprint Lithography (NIL) firstly in 1995[1], which has been considered to be one of the supporting technologies for patterning by International Technology Roadmap for Semiconductors (ITRS) since 2003. NIL has been researched extensively and developed quickly due to its many advantages, such as low cost, high yield, simple process, high fidelity, etc. In recent years, the minimum feature size achieved in NIL is 2.4 nm[2], while the resolution ratio with flexible template, which overcomes substrate surface irregularities, reaches 12.5 nm[3]. At present, many kinds of technologies, such as thermoplastics[4], ultrasonic[5], ultraviolet[6], electrostatic[7], gasbag press[8], direct metallic patterning[9], flexible template[3],micro-contact[10], reversal[11], etc, were introduced to NIL. The patterning resist has been extended originally from PMMA to ultraviolet resist, PDMS, metal thin film, Si, metal nanoparticle encapsulated with hexanethiol self-assembled monolayer, etc.

While the fidelity of imprint patterning is very important in NIL, template and resist directly affect imprint patterning. Now Newtonian fluid is mainly used as resist. But Newtonian fluid has the drawbacks of low filling degree of the template and long filling time. For this reason, pseudoplastic metal nanoparticle fluid (PMNF) was proposed as resist. PMNF shows the shear-thinning property under shear stress, which effectively enhances the filling degree of the template and shortens the filling time[12]. And the metal nanoparticles are easily transferred to bulk metallic patterning in low-temperature, which realizes the direct imprint of metal micro-patterning. Besides, gas pressing method, which eliminates the vibration[13], can effectively improve the uniform of pressing force, which also benefits the fidelity of patterning and prolongs the service life of template[14-15] .

When PMNF is used as resist in NIL, three serious problems arise concerning keeping the morphology of transfer patterning. The first is the fracture on the neck of transfer patterning at the beginning of demolding; the second is the slump on the top of transfer patterning because of shear-thinning property when the demolding is finished; the last is the morphology of bulk metal patterning, when the solvent is evaporated and metal nanoparticles are melted. At the beginning of demolding, the bottom of imprint patterning, which connects the resist in the template and the resist on the substrate, suffers from a big stress. Therefore necking even fracture is likely to happen, leading to the damage of imprint patterning. The previous work has solved the problem. The effects of the friction coefficient, the Hamaker constant, the aspect ratios of the patterning, and the size of the metal nanoparticles on the bottom fracture were obtained [16]. The paper mainly analyzes the second problem, and the third problem is under way.

During the demolding, the friction between template and the boundary fluid of patterning results in the shear-thinning of PMNF. When the viscosity of PMNF boundary fluid decreases, parts of the patterning structure may slump, which makes the fidelity of patterning become worse. The patterning microstructure is assumed to be a cube, the length W, the width R and the height H, respectively, where W is decided by the actual patterning that is needed, R ranges from dozens to one hundred nanometers, H is about several hundred nanometers. Because the four uppermost corners of microstructure suffer from edge effects and the longest friction time during the demolding, their shear-thinning extent is the most obvious. When their viscosity is small enough, the fluid starts to flow, and the microstructure slump, which would directly decrease the fidelity and resolution ratio of the patterning.

After demolding the shear-thinning of fluid does not exist anymore due to the disappearance of the friction force. And the viscosity of microstructure returns to its initial value gradually over time. Thus, the moment when the template completely goes away from the microstructure is critical.

2 Slumping model

In order to confirm the shape and size of slumping structure, a slumping model is proposed based on a theoretical fidelity height (TFH). As shown in figure 1(a), the TFH H' starts from the central point of the bottom surface and goes through the central point of the top surface. The lines, which are helpful to ensure the slumping interface, going through the highest point of H' and the nether endpoint of each b which is a part of H from the top are marked by four dotted red line. Take the front-left structure as example, the dotted red line intersects the top surface of microstructure at point E. The section through point E is the interface between the front-left slumping structure and the master-microstructure, which is marked by the blue area S.

The shape and size of slumping structure is determined by pseudoplastic fluid thixotropism and the thinning extent of microstructure edges. At the end of demolding, the viscosity reduction of fluid on the top of microstructure corners is the largest, simultaneously, the viscosity of fluid at the bottom of microstructure decreases, but the reduction is further smaller than the top. The cross-section horizontal length of slumping structure increases from the bottom to the top of the microstructure. Therefore the shape of slumping structure is a tetrahedron. But the size can't be ensure because of many uncertain factors.

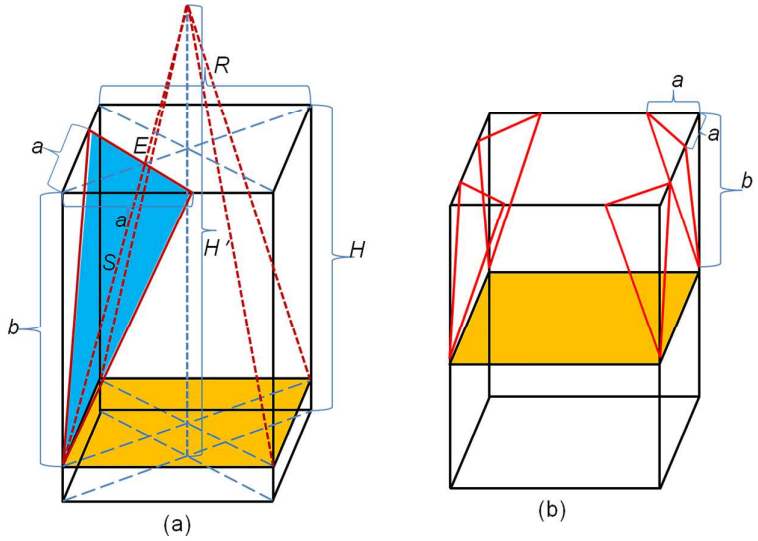

Fig.1 (a) Three-dimension slumping model basing on TFH

(b) Four slumping-bodies of microstructure

The volume of slumping structure increases with the decrease of *H'*, and the shape of four slumping-bodies will become a whole compatible slumping-body when *H'* is short enough. Under the critical condition where the four slumping-bodies precisely begin to roll into one, the right side *a* of the whole slumping-body happens to be equal to half of the width *R* of microstructure, namely *R* /2. Now when the value of *H'* is confirmed, the other right side *b* of the whole slumping-body is solely determined accordingly. Here the critical geometry shape of slumping-body under the value of *H'* is determined. Therefore when *b* is determined, *H'* is greater than the critical value, *a* is smaller than *R* /2, slumping structures are composed of four slumping-bodies, and the higher *H'* is, the smaller *a* is, namely the smaller volume of slumping structures is. When *H'* is smaller than the critical value, all four slumping structures will be an entity, whose upper side is *R*. This represents the most serious slumping state, which brings about the worst fidelity of patterning. Among all the cases, when *a* is smaller than *R* /2, the slumping is the slightest. In this case, when *H'* is greater, the demolding process is better in NIL. In theory, *H'* can be an arbitrary value from (*H*-*b*) (as *b* equals to *H*, (*H*-*b*) equals to zero) to infinity. When *H'* is close to infinity, the slumping interfaces will overlap with the lateral surfaces of microstructure, namely no slumping appears during demolding, and now the fidelity of patterning is the most optimal.

In NIL, the slumping can not be permitted even in the most possible slumping case where *a* is lower than *R*/2. Under the condition, no slumping of microstructure is studied in the literature. The integral slumping structures are shown in figure 1(b), which are called slumping-body with four tetrahedrons. And the tetrahedron is composed of three right triangle faces and an isosceles triangle face. Furthermore, the lengths of the two top right sides of the tetrahedron are equal because of the equal shear-thinning effect and assumed as *a* , and the third right side is assumed as *b*, where $a \le W$ and $a \le R$, then $b \le H$.

3 Simulation analysis

The process of demolding in NIL is simulated with COMSOL Multiphysics. On the edge of two-dimension microstructure, five points are selected, as shown in figure 2. The initial viscosity

of PMNF is set as 166 Pa•s, and the demolding velocity is 100 nm/s. The fluid viscosity changes of these points during demolding are shown in figure 3.

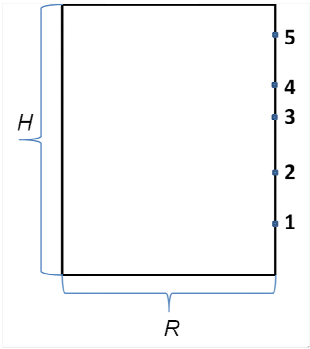

Fig.2 The selected points on the edge of two-dimension microstructure

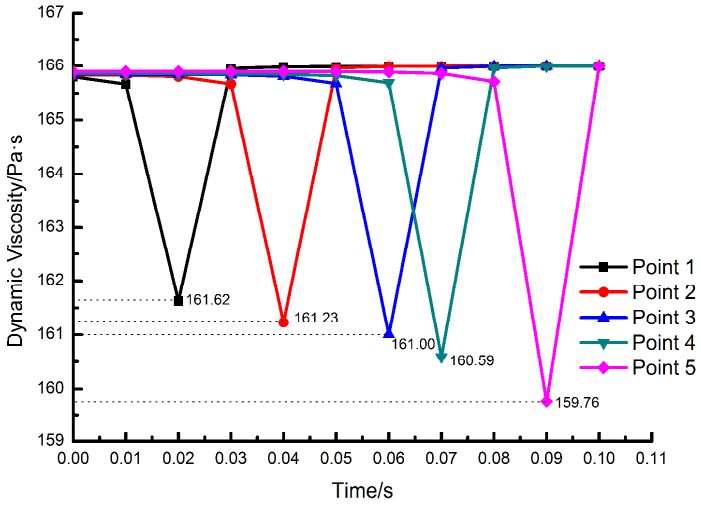

Fig. 3 The fluid viscosity of the five edge points

It can be seen that in figure 3, the fluid viscosity at each point firstly decreases, and then increases with time during demolding. The decrease of fluid viscosity is caused by the friction between the template and pseudoplastic fluid. Nevertheless, the viscosity recovers gradually after the template goes away from the fluid. The simulation results under ideal condition show that fluid viscosity nearly recovers to its initial value. However, in fact, due to its thixotropy the viscosity of pseudoplastic fluid is hard to recover up to the initial value during such a short demolding time .

But beyond that, figure 3 shows that the reduction of the viscosities from point 1 to point 5 continuously increases during the demolding. Namely, there is a shear-thinning strengthening tendency from the bottom to the top along the microstructure edges, which is caused by the adding of friction time. The viscosity of the four top corners of microstructure is the smallest and the fluid in these areas is likely to flow after demolding, which will lead to patterning slumping. The simulation results are consistent with theoretical expectation, and the slumping model proposed is reasonable.

4 The influence of PMNF parameters

When demolding is finished, the fluid in the four vertices of microstructure has the minimum viscosity and the strongest tendency to flow. When the viscosity of vertice fluid reaches the

threshold value, the fluid begins to flow. The fluid containing the vertice fluid with a tendency to flow is called slumping-body, and the remaining fluid of microstructure is called master-microstructure. The separatrix surface between slumping-body and master-microstructure is called slumping interface, which is shown by red line in figure 1(b). But the viscosities of fluid form a viscosity gradient on the horizontal section of microstructure, and gradually become larger as the deepness grows from the boundary to the center of the microstructure. The slumping interface must lie in the gradient fluid. And the slumping-interface actually may be not a plane because of the character of PMNF.

4.1 Slumping interface

PMNF could be prepared by uniformly mixing metal nanoparticles with different sizes that range from 1 to 5 nm in precursor solution. When the slumping-body slides relative to the master-microstructure, there are three situations of metal nanoparticle distribution on the interface: (I)There are no metal nanoparticles on the slumping-interface. (Π)There are metal nanoparticles on the slumping-interface, and most volume of a metal nanoparticle is in the slumping-body. (Ш)There are metal nanoparticles on the slumping-interface, but most volume of a metal nanoparticle is in the master-microstructure. A cross-section view of microstructure about the metal nanoparticle distribution is shown in figure 4(a). When slumping-body slides, metal-nanoparticle *c* and *d* will go with it, but metal-nanoparticle *e* is stationary staying in master-microstructure. The height of a metal nanoparticle inlaying in the relative moving fluid is assumed as *h*. If *h* is determined, the friction force between the relative moving fluid and metal nanoparticle is certain , which is true not only in situation Π but also in situation Ш.

According to Amonton law, the static friction force on the contact surface between metal nanoparticle and the fluid is:

$$f = \mu_s F_N \tag{1}$$

where μ_s is the static friction coefficient, which relates to the surface roughness of metal nanoparticle. F_N is the normal stress that acts on the contact surface S_0. As for the contact between metal nanoparticle and precursor solution, the normal stress is van der Waals force $F_{Au\text{-}f}$, and the expression is[16]:

$$F_{Au-f} = \frac{A_{23}}{6\pi Z_0^{\,3}} \cdot S_0 = \frac{A_{23} r h}{3 Z_0^{\,3}} \tag{2}$$

where r is the radius of a metal nanoparticle, h ($0 \le h \le r$) is the height that a metal nanoparticle inlays in the relative moving fluid, shown in figure 4(b), A_{23} is the Hamaker constant while metal nanoparticle contacts with precursor solution, Z_0 is atomic separation between metal nanoparticle and precursor solution.

So the static friction force is:

$$f = \mu_s \frac{A_{23} r h}{3 Z_0^{\,3}}$$

The static friction force f is proportional to h, and when h is close to zero, f should reach its minimum value. Here it is reasonable to suppose that no metal nanoparticles exist on the slumping-interface, as in situation I.

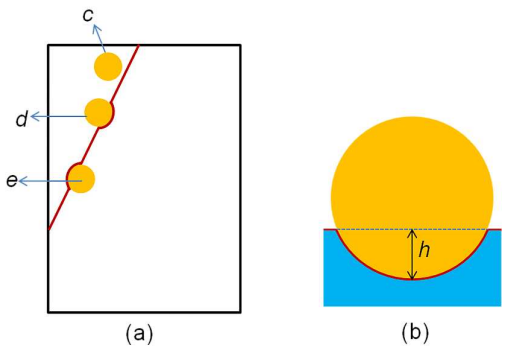

Fig.4 (a) Metal nanoparticle distribution on the slumping-interface
(b) The diagram of a metal nanoparticle inlaying in precursor solution

As known from the above discussion, the slumping-body is likely to slide when no metal nanoparticles exist in the slumping-interface. In the case, the parameters are calculated to guarantee slumping-body no sliding. And these parameters are applicable to the other two cases. Then the following force analysis aims at case I, and the critical relevant parameters of microstructure with no slumping during demolding are obtained.

4.2 The analysis of forces

Because the microstructure is axisymmetric and four corners suffer from equivalent shear force and the same length of time during demolding, the viscosity changes of the four slumping-bodies are the same. The front-left slumping-body marked as *ABCD* is chosen as the example for analysis. After demolding, slumping-body bears the following forces: three atmospheric pressure forces f_{P1}, f_{P2}, f_{P3}, which act on the three right triangle surfaces, surface tension force F_s, intermolecular force F_i between slumping-body and master-microstructure, slumping-body gravity G, normal force N on the contact interface, and viscous force F_v. These forces are shown in figure 5. Only the forces whose orientations are parallel to cant *BCD* do contribute to the sliding of slumping-body, and the forces perpendicular to cant BCD are ignored.

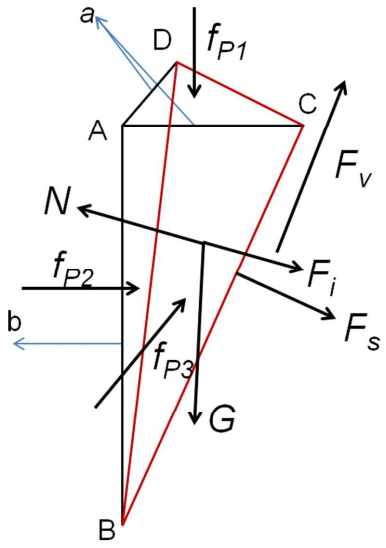

Fig.5 Force analysis of slumping-body

4.2.1 Atmospheric pressure forces

After demolding, the microstructure is out of the vacuum chamber, and the slumping-body is exposed to air. Its three surfaces suffer from the atmospheric pressure forces, namely f_{P1}, f_{P2}, f_{P3}, which turn towards vertical orientation and inwards of the three right triangle planes, respectively. $f_{P1} = P \bullet S_1$, $f_{P2} = P \bullet S_2$, $f_{P3} = P \bullet S_3$, where P is the atmospheric pressure and S_1, S_2, S_3 are the stress-bearing surfaces, $S_1 = a^2/2$, $S_2 = S_3 = (a \bullet b)/2$. In figure 5, it can be seen that the three atmospheric pressure forces are not on the cant BCD. As shown in figure 6(a), $f'_{P1}, f'_{P2}, f'_{P3}$ are the projection forces of f_{P1}, f_{P2}, f_{P3} on cant BCD. And f'_{P1} is parallel down to cant BCD while f'_{P2} and f'_{P3} are respectively parallel up to BCD at the angle θ_1, θ_2, and $f'_{P2} = f'_{P3}$, $\theta_1 = \theta_2$. Then the components f'_{P21}, f'_{P22} of f'_{P2}, and the components f'_{P31}, f'_{P32} of f'_{P3} are obtained in figure 6(b). f'_{P22} and f'_{P32} are parallel up to cant BCD and their directions are the same. f'_{P31} and f'_{P32} are parallel to line CD ,which are equal in magnitude but opposite in the direction.

$$f'_{P1} = \frac{a^2 bP}{2\sqrt{\frac{a^2}{2} + b^2}}, \quad f'_{P22} = f'_{P32} = \frac{a^2 bP}{4\sqrt{\frac{a^2}{2} + b^2}}$$

Therefore, the resultant force parallel to BCD is:

$$F_P = f'_{P1} - (f'_{P22} + f'_{P32}) = 0 \tag{3}$$

That is to say, the atmospheric pressure forces have no contribution to the sliding of slumping-body.

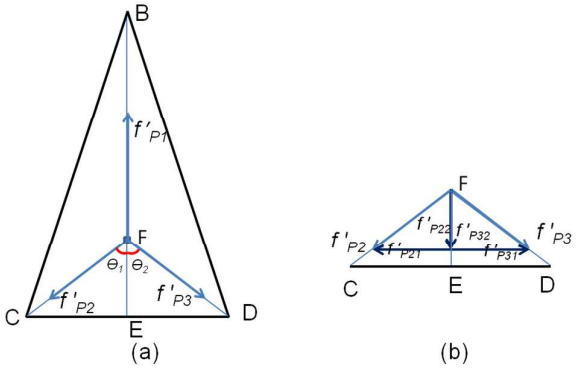

Fig.6 (a)The projections of three atmospheric pressure forces

(b)The components of f'_{P2} and f'_{P3}

4.2.2 Gravity

Gravity that acts on slumping-body can be expressed $G = m \bullet g = \rho \bullet V \bullet g$, where ρ is the density of PMNF, V is the slumping-body volume, $V = (a^2 b)/6$, $g = 9.8\ N/Kg$. The component force $G_{//}$ parallel down to cant BCD is:

$$G_{//} = \frac{a^2 b^2}{6\sqrt{\frac{a^2}{2} + b^2}} \rho g \tag{4}$$

4.2.3 Surface tension force

The liquid molecules on the surface have a tendency to move towards the inner due to the unbalanced intermolecular force, which leads to surface tension forces on the circumference line of the contacting interface. The forces are consecutive on the line, tangent to the liquid surface and

perpendicular to the separatrix line. Surface tension force is:

$$F_s = \sigma \cdot l \tag{5}$$

where σ is surface tension coefficient, namely surface tension force per unit length, and is related to fluid property. l is the length of circumference line. As shown in figure 5, the sliding surface of slumping-body is the cant *BCD*, and the tangent surfaces are plane *ABC*, plane *ACD*, and plane *ABD*, respectively. So surface tension force can be calculated separately:

$$\vec{F}_s = \vec{F}_1 + \vec{F}_2 + \vec{F}_3 \tag{6}$$

$$F_1 = \sigma \cdot l_{BC}, \quad F_2 = \sigma \cdot l_{CD}, \quad F_3 = \sigma \cdot l_{BD}$$

F_1 is perpendicular to line *BC* on plane *ABC*, F_2 is perpendicular to line *CD* on plane *ACD*, F_3 is perpendicular to line *BD* on plane *ABD*. The directions of all forces are against the slumping-body. The three forces are resolved and composed in the direction parallel to cant *BCD*, and the resultant force $F_{s//}$ is

$$F_{s//} = \frac{\sigma a(b-a)}{\sqrt{\frac{a^2}{2} + b^2}} \tag{7}$$

with its orientation parallel down to cant *BCD*.

4.2.4 Intermolecular force

Slumping-body which contains precursor solution and metal nanoparticles suffers from intermolecular force provided by master-microstructure. The intermolecular force is composed of four parts: $F_{f\text{-}f}$ between precursor solution in master-microstructure and precursor solution in slumping-body, $F_{Au\text{-}f}$ between metal nanoparticles in master-microstructure and precursor solution in slumping-body, $F_{f\text{-}Au}$ between precursor solution in master-microstructure and metal nanoparticles in slumping-body, and $F_{Au\text{-}Au}$ between metal nanoparticles in master-microstructure and metal nanoparticles in slumping-body, respectively. There's no doubt that $F_{f\text{-}f}$ is perpendicular to cant *BCD*. And yet, intermolecular force, namely adhesion force, between metal nanoparticles and precursor solution only exists on the contact surface, so $F_{Au\text{-}f}$ and $F_{f\text{-}Au}$ are both perpendicular to cant *BCD*.

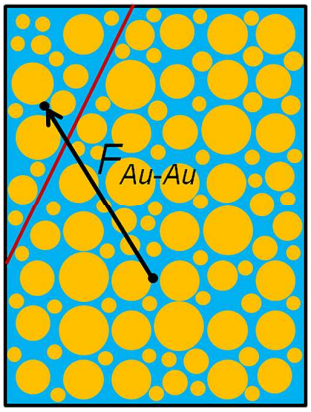

Fig.7 The intermolecular force between metal nanoparticles

Metal nanoparticles with different sizes are distributed uniformly in precursor solution.

Hence, it is hard to calculate $F_{Au\text{-}Au}$ of each metal nanoparticle in slumping-body which is provided by all metal nanoparticles in master-microstructure. All metal nanoparticles in slumping-body are supposed as an entity, and all metal nanoparticles in master-microstructure are another entity. And their centers of mass are respectively on its own geometric center. $F_{Au\text{-}Au}$ between the two entities is on the line through the two centers of mass, as shown in figure 7. Au nanoparticles are used in the calculation, the mass of metal nanoparticles in slumping-body is M_1, and the mass of metal nanoparticles in master-microstructure is M_2. Therefore, $F_{Au\text{-}Au}$ between the two entities is

$$F_{Au-Au} = \frac{GM_1M_2}{R_0^{\ 2}} \tag{8}$$

where G is universal gravitational constant, R_0 is the distance between the two centers of mass. The volume ratio of metal nanoparticles in PMNF is assumed as 70%, so

$$M_1 = \frac{1}{6}a^2b \times 70\% \times \rho_{Au} \times g$$

$$M_2 = RHW \times 70\% \times \rho_{Au} \times g - 4M_1$$

$F_{Au\text{-}Au}$ is much less than other forces based on calculation, so it is negligible to the resultant force.

4.2.5 Viscous force

When slumping-body has a tendency to flow, it will be prevented by internal friction force namely viscous force on the slumping-interface. The viscous force is decided by the property of precursor solution as no metal nanoparticles exist on the slumping-interface. And it is expressed in the following according to the generalized Newton internal friction law.

$$F_v = S\tau \tag{9}$$

$$\tau = \eta\gamma$$

Here τ is shear force per unit area of fluid; S is the area of sliding cant, $S = \frac{a\sqrt{a^2+2b^2}}{2}$; η is the viscosity of fluid on the slumping-interface; γ which is called shear rate stands for the velocity gradient perpendicular to the flowing direction, $\gamma = dV/dy$, dy is thickness of an infinitely thin fluid layer, while d_V is velocity increment on the distance of dy.

According to the power-law equation of fluid, $\eta = K \cdot \gamma^{n-1}$, K represents consistency coefficient and n stands for power law index, which can also be called rheological index. The viscous force is:

$$F_v = \frac{a\sqrt{a^2+2b^2}}{2} \times \sqrt[n-1]{\frac{\eta^n}{K}} \tag{10}$$

with its orientation parallel up to cant *BCD*.

4.3 The analysis of critical state

Through the analysis above, only gravity G, surface tension force F_s, and viscous force F_v contribute to the sliding of slumping-body. In order to prevent slumping-body from sliding, these forces should meet the relation:

$$F_{s//} + G_{//} \le F_v \tag{11}$$

Then the expressions of all forces are put into Eq.11,

$$\frac{\sigma a(b-a)}{\sqrt{\frac{a^2}{2}+b^2}}+\frac{a^2b^2}{6\sqrt{\frac{a^2}{2}+b^2}}\rho g \le \frac{a\sqrt{a^2+2b^2}}{2}\times\sqrt[n-1]{\frac{\eta^n}{K}}$$

It can be simplified as

$$\eta \ge \left\{K\left[\frac{6\sqrt{2}\sigma(b-a)+\sqrt{2}ab^2\rho g}{3(a^2+2b^2)}\right]^{n-1}\right\}^{\frac{1}{n}} \tag{12}$$

After demolding, no slumping appears in the microstructure only when the viscosity of fluid on the slumping-interface is satisfied with Eq.12. Here in order to clarify the description, η_c is used to represent the summation of the complex expression. So the expression is:

$$\eta_c = \left\{K\left[\frac{6\sqrt{2}\sigma(b-a)+\sqrt{2}ab^2\rho g}{3(a^2+2b^2)}\right]^{n-1}\right\}^{\frac{1}{n}}$$

The influences of a and b on critical viscosity η_c with other parameters as constants under different initial viscosities of PMNF are discussed, and the curve graphs are shown in figure 8.

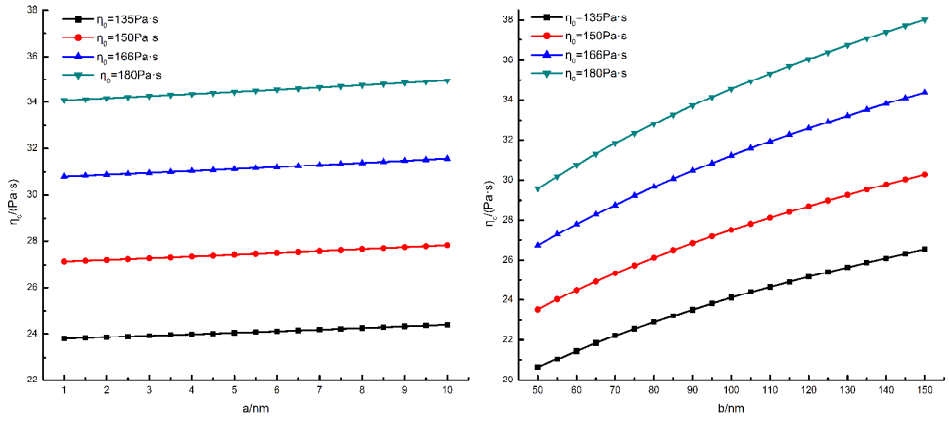

Fig.8 The influences of a and b with different initial viscosities

In figure 8, if a is certain, the critical viscosity η_c after demoding is bigger when initial viscosity η_0 is bigger. And the phenomenon is also applied to b. When initial viscosity η_0 is fixed, η_c is observed to increase with the increase of a or b. Once again it is validated that the viscosity changes of the fluid which are closer to the centre of microstructure are smaller. And the increase extent of η_c is more obvious for b, that is to say, the influence of friction force on the edge is bigger than the accumulated effect in the microstructure.

When the size of slumping-body is smaller than one tenth of feature size of imprinting microstructure patterning, the influence of slumping on the fidelity of patterning can be negligible. Assume that $a = 6\ nm$, $b = 100\ nm$, the influences of four attribute parameters of PMNF (consistency coefficient K, rheological index n, density ρ, and surface tension coefficient σ) on the

critical viscosity η_c after demolding are researched.

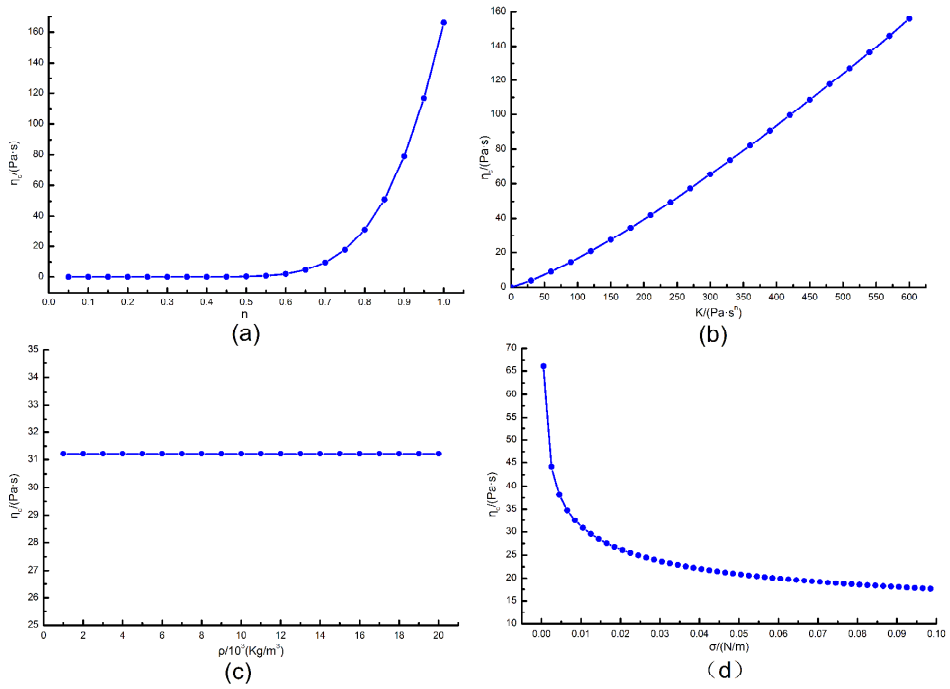

Fig.9 The critical viscosity η_c with rheological index n, consistency coefficient K, density ρ, surface tension coefficient σ

The effect of rheological index n on critical viscosity η_c is shown in figure 9(a). Assume that $K = 166\ Pa{\bullet}s^n$, $\sigma = 0.01\ N/m$, $\rho = 13.81\times10^3\ Kg/m^3$. η_c is observed to increase with the increase of n. When $n<0.6$, η_c changes slowly; when $n>0.6$, the increase tendency is obvious. When n approaches 1, η_c is close to the initial viscosity 166 Pa•s. Because fluid doesn't have the property of pseudoplastic as n is 1. Only when n is smaller than 1, is the fluid pseudoplastic fluid. The smaller n is, the stronger pseudoplastic is. In order to enhance the filling degree of template, great liquidity fluid with small n is expected. Simultaneously, when n is small, η_c that is gotten after demolding is small, too. And smaller η_c is easier to meet Eq. 12 for demolding technology, which can ensure good fidelity of microstructure. However, too small n will increase the difficulty and cost to fabricate PMNF.

The effect of consistency coefficient K on critical viscosity η_c is depicted in figure 9(b). Assume that $n = 0.8$, $\sigma = 0.01\ N/m$, $\rho = 13.81\times10^3\ Kg/m^3$. It can be seen that η_c increases with the increase of K, and the curve diagram is similar to linear relationship. Similarly, the theoretical η_c gotten from the Eq.12 is expected to be small, which means that smaller K should be taken. But K is linked with initial viscosity η_0, and a large η_0 is helpful to keep the patterning morphology when it is static. Taking the two factors into account, K can be confirmed.

The curve of critical viscosity η_c versus density ρ is drawn in figure 9(c). Assume that $n = 0.8$, $\sigma = 0.01\ N/m$, $K = 166\ Pa{\bullet}s^n$. η_c has little change with the increase of ρ. It can be considered η_c is independent from ρ. When pseudoplastic fluid is fabricated, the influence of ρ can be ignored.

The curve of critical viscosity η_c versus surface tension coefficient σ is drawn in figure 9(d). Assume that $n = 0.8$, $\rho = 13.81\times10^3\ Kg/m^3$, $K = 166\ Pa{\bullet}s^n$. It can be seen that η_c decreases with

the increase of σ, and when σ is smaller, η_c changes obviously, but tends to be a stable value finally as σ is big enough. The factor of small theoretical η_c is considered and larger σ is taken. σ is linked with ρ, and the larger ρ is, the larger σ is. But only when PMNF contains more metal nanoparticles will ρ be large, which will also lead to much more difficulty and cost to fabricate PMNF.

5 The influence of demolding velocity

The parameters of PMNF affecting the slumping-interface viscosity η are determined. And their influences on η are indirect. The friction between template and edges of microstructure during demolding, leads to the marginal PMNF shear-thinning. And the thinning extent of PMNF varies with the demolding velocity. The bigger demolding velocity is, the bigger shear-thinning extent is. So demolding velocity directly affects the slumping-interface viscosity η. And demolding velocity must not be bigger than the critical value, whose corresponding viscosity η meets Eq.12.

5.1 The velocity of boundary layer

At the beginning of demolding process, the template is pulled up, and has the velocity V_t instantly. During the process, the template is kept moving uniformly with the speed V_t by varying the pull. Because the movement is relative, suppose that the value of template velocity is zero, the numerical value of microstructure velocity V_m will be equal to V_t, but V_m has the opposite direction with V_t, namely $\boldsymbol{V_m} = - \boldsymbol{V_t}$.

When fluid contacts with solid wall, it sticks to the solid wall, and the velocity of the adhesive fluid layer is zero. But the velocity of fluid near the center of microstructure is V_m. A separatrix must exist in the microstructure, and the velocity of fluid on the side close to template of separatrix is smaller than V_m, while that on the other side of separatrix is equal to V_m. So the fluid layers, which is located in different position between the separatrix and template, have different velocities which result in relative motions. The fluid with relative motions is called boundary layer of velocity, and its thickness is assumed as δ. The inner frictions in the boundary layer of velocity, which is caused by the relative motions, lead to the fluid shear-thinning. Then the viscosity of fluid is smaller than η_0, and the closer to template the fluid is, the smaller viscosity is. The fluid in boundary layer has a viscosity gradient. In fact, the separatrix is difficult to be identified, as δ tends to be infinite when the velocity of fluid on the separatrix is entirely equal to V_m. In general, if the velocity of fluid on the separatrix reaches 99.5%V_m, the separatrix is accepted, and the thickness of boundary layer is called δ(995). The boundary layer model of laminar flow can be used to analyze the relative motions between template and microstructure during demolding. The model is shown in figure 10[17]. The velocity gradient of fluid layer becomes larger when the fluid is closer to the template. The positive direction of x-axis stands for the contact surface upward between template and microstructure; and the positive direction of y-axis stands for the direction vertical to the contact surface with microstructure inwards. When y is zero, it is the position of template.

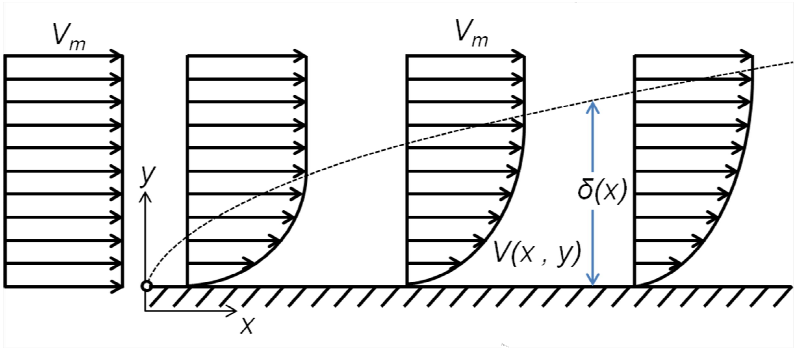

Fig.10 The model of velocity of boundary layer

Because the shear-thinning effects of fluid are accumulated with the friction time. The thickness of boundary layer increases along with the lasting of separation movement between template and microstructure, namely δ increases with the increase of y. The thickness of fluid layers whose viscosities decrease increases with the increase of y. The four possible slumping-bodies on the edge of microstructure appear to the quadrihedron shape, just as figure 1(b) shows.

5.2 Slip velocity

The fluid adjacent to template has a phenomenon of adhesion or separation now and then with template during demolding. Knudsen (Kn) of the moving region has the order of 10^{-2}, which means that the movement belongs to slipping movement, and relative motion exists on the solid-liquid surface. The velocity of fluid on the template is no longer zero shown in figure 10, but is the slip velocity V_s shown in figure 11(a). However, velocity gradient in the horizontal section of microstructure still exists. The expression [18-19] of slip velocity is:

$$V_s = B\frac{\partial V(x,y)}{\partial y}\Big/_{wall} \tag{13}$$

where B is slip length, which stands for the distance between the virtual solid-liquid surface and the actual one. And the slip velocity is zero on the virtual solid-liquid surface. $V(x, y)$ is fluid velocity.

Relative motions between different fluid layers lead to the decrease of fluid viscosity. So the velocity boundary layer is the viscosity boundary layer at the same time. The viscosity boundary layer is supposed to be divided into N ($1, 2... i$ ...) layers uniformly, as shown in figure 11(b). The interface between two adjacent fluid layers is considered parallel to the slumping-interface, and the fluid layer adjacent to template has the minimum viscosity. The initial viscosity of PMNF is η_0, and the average value of viscosity of each layer is taken. From the internal microstructure, the viscosity of the first layer is η_1, the second layer is η_2, and so on, and the last layer in touch with template is η_N. The fluid containing layer $(i+1)$ begins to flow when η_i is small enough. Here the viscosity of fluid on the interface is η_i, and the fluid layer whose viscosity is η_i is in the master-microstructure. The interface between the layer i and the layer $(i+1)$ is slumping-interface, so η_i is the slumping-interface viscosity η. Therefore slip length B[19-20] can be expressed as:

$$B = d(\frac{\eta_{N-1}}{\eta_N} - 1) = \frac{a}{(N-i)}(\frac{\eta_{N-1}}{\eta_N} - 1) \tag{14}$$

where $d = a/(N-i)$ is the thickness of one fluid layer and a is the length of one right side of the

slumping-body. Hence, the thickness of the whole velocity boundary layer is $\delta = (aN)/(N-i)$.

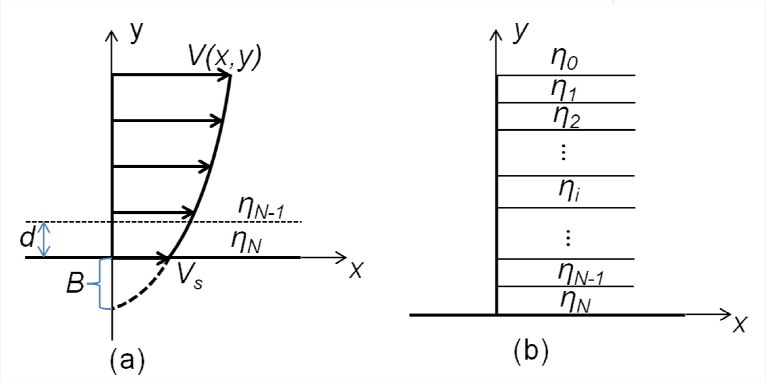

Fig.11 (a) The model of slip velocity (b)The layers of viscosity boundary layer

5.3 The analysis of demolding velocity

Velocity gradient exists in the velocity boundary layer and velocity gradient has a gradient itself, which is assumed as C. According to the viscosity feature of boundary layer, C, which is negative, is related to the fluid character and x which stands for the altitude of fluid in the microstructure. When PMNF is determined, $C(x)=\frac{\partial^2 V}{\partial y^2}$. The altitude of fluid is higher, the velocity variation is larger and the relative motion is fiercer, so the reduction of viscosity is greater. When $x = H$, fluid has the minimum viscosity. Suppose that $C(H) = C_0$, the velocity variation of velocity boundary layer of the thin fluid layer containing the upper surface of microstructure is researched. The velocity is assumed as:

$$V=\alpha y^2+\beta y+\varepsilon \tag{15}$$

and

$$\begin{cases} \frac{\partial^2 V}{\partial y^2}\Big/_{x=H}=C_0 \\ \frac{\partial V}{\partial y}\Big/_{y=\frac{aN}{N-i}}=\gamma_0 \\ V\Big/_{y=0}=V_s \end{cases}$$

where γ_0 is the shear rate matching η_0, then $\alpha=\frac{1}{2}C_0$, $\beta=\gamma_0-\frac{aNC_0}{N-i}$, $\varepsilon=V_s$.

The fluid velocity is obtained:

$$V=\frac{1}{2}C_0y^2+(\gamma_0-\frac{aNC_0}{N-i})y+V_s$$

And $V_s=B\frac{\partial V}{\partial y}\Big/_{y=0}$, so

$$V_s=B(\gamma_0-\frac{aNC_0}{N-i})$$

$$V_s=\frac{a}{N-i}(\frac{\eta_{N-1}}{\eta_N}-1)(\gamma_0-\frac{aNC_0}{N-i})$$

That $\frac{\partial V}{\partial y}/_{y=d} = \gamma_{N-1}$, $\frac{\partial V}{\partial y}/_{y=0} = \gamma_N$, $\frac{\partial V}{\partial y}/_{y=a} = \gamma_i$, $\eta = K\gamma^{n-1}$, the expressions are:

$$\eta_{N-1} = K\left[\gamma_0 - \frac{aC_0}{N-i}(N-1)\right]^{n-1} \tag{16}$$

$$\eta_N = K(\gamma_0 - \frac{aNC_0}{N-i})^{n-1} \tag{17}$$

$$\eta_i = K(\gamma_0 - \frac{aiC_0}{N-i})^{n-1} \tag{18}$$

$$C_0 = \frac{\gamma_0 - (\frac{\eta_i}{K})^{\frac{1}{n-1}}}{\frac{ai}{N-i}} \tag{19}$$

Then Eq.16 and Eq.17 are put into Eq.15. Therefore Eq.20 is

$$V_m = V/_{y=\frac{aN}{N-i}} = \frac{1}{2}C_0(\frac{aN}{N-i})^2 + (\gamma_0 - \frac{aN}{N-i}C_0)(\frac{aN}{N-i}) + \frac{a}{N-i}\left\{\frac{K\left[\gamma_0 - \frac{aC_0}{N-i}(N-1)\right]^{n-1}}{K(\gamma_0 - \frac{aNC_0}{N-i})^{n-1}} - 1\right\}(\gamma_0 - \frac{aN}{N-i}C_0) \tag{20}$$

And the expression C_0 is replaced,

$$V_m = \frac{aN^2}{2i(N-i)}\left[\gamma_0 - (\frac{\eta_i}{K})^{\frac{1}{n-1}}\right] + \frac{aN\left[N(\frac{\eta_i}{K})^{\frac{1}{n-1}} - (N-i)\gamma_0\right]}{i(N-i)} + \frac{a\left[N(\frac{\eta_i}{K})^{\frac{1}{n-1}} - (N-i)\gamma_0\right]}{i(N-i)}\left[\frac{(N-1)(\frac{\eta_i}{K})^{\frac{1}{n-1}} - (N-i-1)\gamma_0}{N(\frac{\eta_i}{K})^{\frac{1}{n-1}} - (N-i)\gamma_0} - 1\right] \tag{21}$$

where η_i is the slumping-interface viscosity η. Assume that consistency coefficient $K = 166\ Pa{\bullet}s^n$, rheological index $n = 0.8$, $a = 6$ nm, $N = 10$, $i = 3$, and initial viscosity η_0 is 135 Pa•s, 150 Pa•s, 166 Pa•s, 180 Pa•s, respectively, the graphs of slumping-interface viscosity η and demolding velocity V_m can be calculated and shown in figure 12. If demolding velocity is the same, initial viscosity η_0 is larger, the slumping-interface viscosity η gotten after demolding is larger. When initial viscosity η_0 is determined, slumping-interface viscosity η decreases with the increase of demolding velocity V_m. Furthermore, when initial viscosity η_0 is bigger, the reduction is more obvious. It's known from the discussion above, the larger viscosity of slumping-interface can better prevent slumping-body from sliding. Demolding velocity must be reduced to prevent the patterning from slumping.

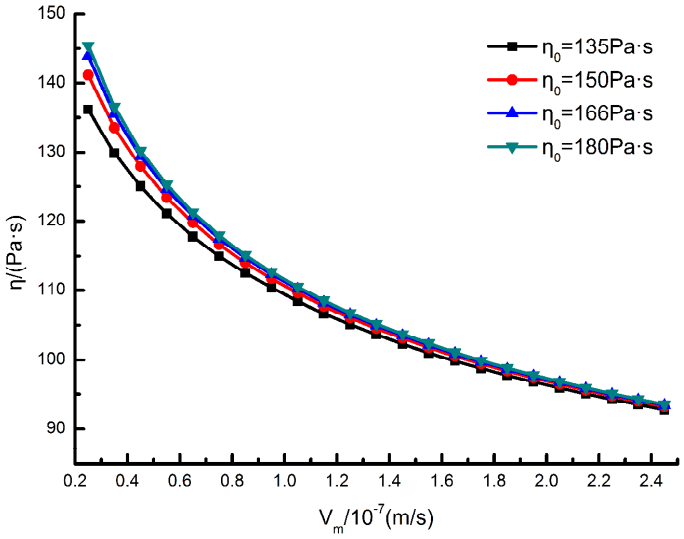

Fig.12 The critical viscosity with demolding velocity

6 Conclusions

By taking advantage of the shear-thinning of PMNF, the filling degree of the template is improved, and the metal patterning can be realized directly in NIL. However, in order to optimize the service life of template and the processing time, demolding should be carried out in a short time after imprinting. The shear-thinning of PMNF which is used as resist during demolding will affect the integrity of patterning. By analyzing the possible slumping-body, these coefficients and physical parameter are obtained under the worst situation where fluid is likely to slide. In order to avoid the appearance of slumping, smaller consistency coefficient, smaller rheological index and larger surface tension coefficient should be selected, and the demolding velocity ought to be reduced. These conclusions provide significant theoretical guidance for the fabrication of PMNF and the demolding process in NIL.

Acknowledgments

This work is sponsored by the National Natural Science Foundation of China (Grant No. 51175479), and the Education Department of Henan Province, China. (Grant No.13A460725, 2013GGJS-001). The authors would like to thank Dr. B. Cai for the paper polishing.

References

[1]. S. Y. Chou, P. R. Krauss, and P. J. Renstrom. *Science*, 1996, 272(5258), 85-87.

[2]. F. Hua, Y. Sun, A. Gaur, M. A. Meitl, L. Bilhaut, L. RotKina, et al. *Nano Letters*, 2004, 4(12), 2467–2471.

[3]. G. Kreindl, M. Kast, D. Treiblmayr, T. Glinsner, et al. *Proc. of SPIE*, 2011, 7970, 79701.

[4]. H. Yoon, H. S. Cho, K. Y. Suh and K. Char, *Nanotechnology*, 2010, 21,105302.

[5]. H. Mekaru and M.Takahashi, *Journal of Micromechanics and Microengineering*, 2009, 19, 125026.

[6]. J. Perumal, T. H. Yoon, H. S. Jang, J. J. Lee and D. P. Kim, *Nanotechnology*, 2009, 20,

055704.

[7]. H. Hocheng and T. T. Wen, *Microelectron. Eng.*, 2008, 85, 1652-1657.

[8]. F. Cheng, S. Y. Yang, S. C. Nian, and L. A. Wang, *J. Vacuum Sci. Technol. B, Microelectron. Nanometer Struct.*, 2006, 24, 1724-1727.

[9]. S. H. Ko, I. Park, H. Pan, C. P. Grigoropoulos, A. P. Pisano, C. K. Luscombe and J. M. J. Fre´chet, *Nano letters*, 2007, 7, 1869.

[10]. X. M. Zhao, Y. Xia and G. M. Whitesides, *J. Mater. Chem.*, 1997, 7(7), 1069-1074.

[11]. Y.Tsuji, M. Yanagisawa, H. Yoshinaga and K. Hiratsuka, *Journal of Physics:Conference Series*, 2009, 191, 012010.

[12]. W. W. Xia, G. H. Zheng, T. H. Li, C. R. Liu, D. X. Li, Z. Y. Duan. *Acta Phys. sin.*, 2013, 62(18), 188105.

[13]. C. R. Liu, J. Z. Yue, T. H. Li, W. W. Xia, D. X. Li, Z. Y. Duan. *Journal of Mechanical Engineering Science*, 2013 (DOI: 10.1177/0954406213508755.)

[14]. T. H. Li, G. H. Zheng, C. R. Liu, W. W. Xia, D. X. Li, Z. Y. Duan. *IEEE Transaction on Nanotechnology*, 2013, 12(4), 589-595.

[15]. T. H. Li, G. H. Zheng, C. R. Liu, W. W. Xia, D. X. Li, Z. Y. Duan. *Acta Phys. sin.*, 2013, 62(6), 068103.

[16]. W. W. Xia, Y. F. Su, T. H. Li, C. R. Liu, D. X. Li, Z. Y. Duan. *RSC Advances*, 2013, 3(39), 17851 – 17859.

[17]. M. Z. Chen. *Beijing: Higher education press*, 2002, 123-130.

[18]. O. I. Vinogradova. *Langmuir*,1995,11, 2213-2220.

[19]. S. G. Hatzikiriakos. *Progress in Polymer Science*, 2012, 37, 624-643.

[20]. C. W. Wu, G. J. Ma, P. Zhou. *Advances in mechanics*, 2008,38(3), 265-292.

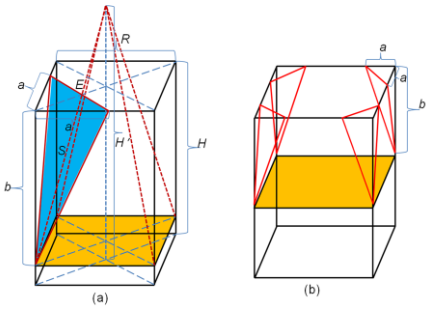

The slumping in nanoimprint lithography with pseudoplastic metal nanoparticle fluid